

WPI Precision Personnel Locator System: Antenna Geometry Estimation Using a Robust Multilateralization Technique

B. Woodacre, D. Cyganski, R. J. Duckworth, V. Amendolare
Worcester Polytechnic Institute, Worcester, Mass.

BIOGRAPHY

Mr. Benjamin Woodacre is a Ph.D. candidate in Electrical and Computer Engineering at WPI. Since completing his MS degree at WPI 2004, he has served as a research assistant in the WPI Convergent Technology Center sponsored by the NIJ/DOJ on the topic of precision personnel location. His MS work examined variation of TDOA localization performance as a function of geometry, and his Ph.D. research concerns techniques for antenna geometry auto-calibration.

Dr. David Cyganski is professor of Electrical and Computer Engineering at WPI where he performs research and teaches linear and non-linear multidimensional signal processing, communications and computer networks, and supervises the WPI Convergent Technology Center. He is an active researcher in the areas of radar imaging, automatic target recognition, machine vision, and protocols for computer networks. He is coauthor of the book *Information Technology: Inside and Outside*. Prior to joining the faculty at WPI, he was an MTS at Bell Laboratories and has since held the administrative positions of Vice President of Information Systems and Vice Provost at WPI.

Dr. R. James Duckworth is an Associate Professor in the Electrical and Computer Engineering department at WPI. He obtained his Ph.D. in parallel processing from the University of Nottingham in England. He joined WPI in 1987. Duckworth teaches undergraduate and graduate courses in computer engineering focusing on microprocessor and digital system design, including using VHDL and Verilog for synthesis and modeling. His main research area is embedded system design. He is a senior member of the IEEE, and a member of ION, IEE, BCS, and is a Chartered Engineer of the Engineering Council of the UK.

ABSTRACT

This paper describes further efforts towards antenna geometry estimation in the WPI Precision Personnel Locator system, which is under development as a portable, zero-fixed-infrastructure, and spectrally compliant RF-based system for location and tracking of personnel situated in indoor environments. The system consists of transmitters worn by individuals to be tracked, and receiver hardware which collectively estimates position mounted upon response vehicles. Pursuit of any location solution requires the availability of an estimate of the receivers' antenna positions of sufficient accuracy so

as not to contribute superfluous error to personnel location estimates. By utilizing each receiving antenna temporarily as a transmitter, sufficient information is collected to derive a solution for the antenna positions, however, while these antennas are outdoors, they experience the same multipath effects as the indoor-to-outdoor radio channel and require application of a robust multilateralization technique not considered in the previous paper. This paper presents methods for antenna geometry estimation based on such a technique and will present results, from a number of experimental tests, illustrating antenna location error as well as total system error when driven by such antenna geometry solutions.

INTRODUCTION:

WPI PRECISION PERSONNEL LOCATOR SYSTEM

The Worcester Polytechnic Institute (WPI) Precision Personnel Locator (PPL) system is the result of an ongoing multi-year research and engineering effort to develop a robust real-time positioning and tracking solution for first responders and other personnel in indoor environments. To date, published papers on these efforts have detailed the system concept [1], signal structure and performance bounds [2], [3], hardware design [4], and experimental test results [5] paralleling the development and refinement of the system's hardware realization and signal processing methods.

Figure 1 is an artist's rendition of the PPL concept. To be tracked, personnel carry a transmitter emitting a multicarrier wideband (MC-WB) signal [2], which is sensed by receiving stations fixed upon emergency response vehicles. Upon arrival, the receiving stations form an ad-hoc network and establish a local coordinate system using methods that are the subject of this paper. A previous paper [6] (to which the current paper is a sequel) described initial signal processing efforts towards estimation of the stations' coordinates.

Given the receiving stations' positions and the signals collected at each station, location solutions for each transmitter may be computed and then conveyed to command-and-control software in the hands of the incident commander. Accumulated track data can provide valuable insight into building layout to assist with self-rescue (exit guidance) or search-and-rescue operations. Beyond being lost or trapped, cardiac distress is also a leading cause of firefighter death [7], and the system incorporates physiological status monitoring into the incident commander's display.

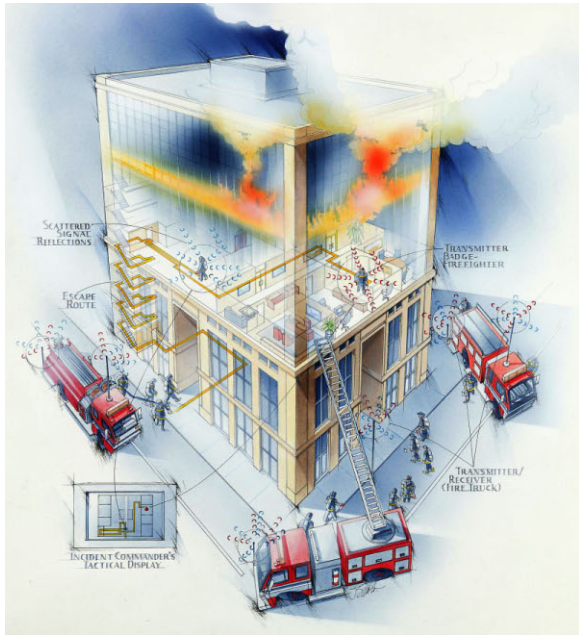


Fig. 1. PPL concept illustration

In the following sections we describe the MC-WB signal, the SART method for robust multilateralization, the problem of geometric antenna configuration (GAC), and methods for the solution of GAC. The performance of these methods is presented in terms of antenna location error as well as impact upon the final transmitter location estimates desired. Throughout the paper the terms *receiver*, *station*, and *antenna* are used interchangeably to refer to the fixed points of signal reception used for positioning, despite their transmit capability during GAC; *transmitter* refers to the individual being located.

Signal Structure

The MC-WB signal consists of a collection of N discrete, unmodulated sub-carriers, each of negligible bandwidth, spread throughout a bandwidth of operation B Hz, spaced at B/N Hz [2]. An example of our current multicarrier signal (at baseband frequencies) viewed on a spectrum analyzer can be seen in Figure 2, where approximately 100 sub-carriers are spread over a 150 MHz bandwidth. The carriers are spaced evenly except where deletions have been made to avoid interfering with existing services in our FCC allocated 550-700 MHz experimental band.

While Figure 2 shows a flat power spectrum for the signal, in receiver hardware it is necessary to calibrate out all superfluous hardware effects, signal delays, and timing offsets, so as to give all receivers similar frequency responses. As the SART algorithm, described later, “compares” received multicarrier signals, individual variation of each receiver’s response is undesirable and so is eliminated. A more difficult source of distortion to compensate for is that induced by the receiver’s antennas. While a shared frequency response due to the antennas’ identical design may be compensated for, the unknown position of response vehicles and local area nature

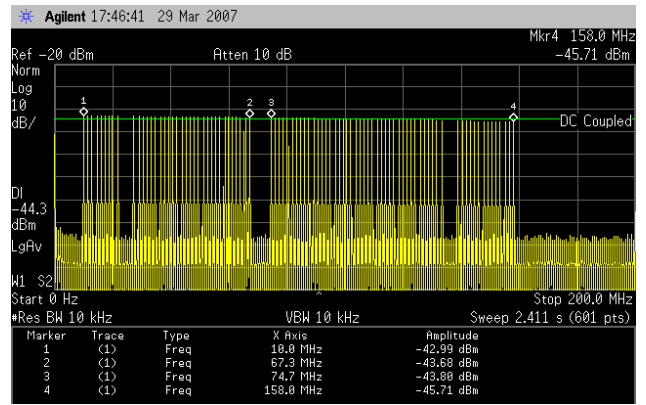


Fig. 2. MC-WB baseband signal spectrum

of the location scenario dictates that the antennas will receive signals from a large diversity of angles. Again, any shared response has no effect on SART processing, but variation in response does, and the diversity of arrival angle at many antennas creates just such a condition. For 2-D positioning with vertical dipole antennas, the effect is negligible, but for other antenna designs and 3-D positioning the effect cannot be ignored. As a first order effect, this distortion due to antenna angle may be modeled as a time delay, as it is the component of the distortion which directly affects the location solution. The antennas currently utilized in the PPL system have been designed with minimization of this effect in mind, such that upon a rotation of 90 degrees, a signal source at a constant distance will show no more than 1 nanosecond (0.3m) of time-delay variation. This distortion due to angle is not an insignificant source of error; however multipath resistance remains the central challenge.

SART

Our group’s initial efforts towards a positioning technology focused on a statistically efficient, model-based [8] estimation procedure for TDOA, but whose accuracy additionally depends on knowledge of parameters of the indoor radio channel, which are generally hard to estimate, such as the number of multipath signals or the identity of the direct path signal. Selecting the direct path signal from a candidate list is at best error-prone: transmitter-receiver asynchrony prevents selection based on earliest arrival time, and building obstructions frequently prevent signal strength from being a reliable indicator.

Singular value array reconciliation tomography (SART) is a new method that has been adopted for the PPL system that avoids the problems of the aforementioned approach and is therefore much more robust. SART avoids intermediate estimates and operates directly with multicarrier signal data from all receivers simultaneously to produce a location solution.

At a particular antenna, the signal measured at the output of a receiver may be written in the frequency domain, sampled at the transmitted subcarrier frequencies $\omega_k = 2\pi f_k$,

$$X(\omega_k) \cdot H(\omega_k) \cdot \sum_i a_i e^{-j\omega_k t_i} \quad (1)$$

where $H(\omega_k)$ is the transfer function of the receiver and $X(\omega_k)$ is the transmitted signal. Assuming these two terms are known, what remains is the channel response containing information about the direct and multipath signal components, each of which is a sinusoid:

$$V(\omega_k) = \sum_i a_i e^{-j\omega_k t_i} \quad (2)$$

where a_i is the amplitude for the i -th signal and t_i determines the periodicity of each signal with respect to ω_k and is the propagation delay of the i -th signal. The SART algorithm assembles the measured channel responses from all antennas into a signal matrix S whose columns are the channel response (2) measured at each antenna,

$$S = \begin{pmatrix} V_1(\omega_1) & \dots & V_n(\omega_1) \\ \vdots & \ddots & \vdots \\ V_1(\omega_k) & \dots & V_n(\omega_k) \end{pmatrix} = D + M. \quad (3)$$

which may be expressed as the sum of direct path signal energy represented by D and multipath signal components in M . While no attempt is made to decompose S into these two terms, the approach taken by SART is to infer the parameters of D (i.e., the signal delays) by manipulating S and observing changes in its rank structure.

Considering direct-path signal energy, the elements of D correspond to phase changes due to line-of-sight propagation at the speed of light:

$$D = a_n e^{-j\omega_k t_n} = \begin{pmatrix} a_1 e^{-j\omega_1 t_1} & \dots & a_n e^{-j\omega_1 t_n} \\ \vdots & \ddots & \vdots \\ a_1 e^{-j\omega_k t_1} & \dots & a_n e^{-j\omega_k t_n} \end{pmatrix} \quad (4)$$

Given knowledge of the antenna positions \vec{p}_n and frequencies ω_k , the received signal may be rephased for a hypothetical source location \vec{x} by removing the appropriate amount of signal delay had the signal originated there:

$$D(\vec{x}) = a_n e^{-j\omega_k t_n} \cdot e^{j\omega_k \|\vec{p}_n - \vec{x}\|_2 / c} \quad (5)$$

where c is the speed of light. Thus the matrix of received signals with propagation delays t_n from a transmitter, rephased to \vec{x} can be written as

$$D(\vec{x}) = a_n e^{-j\omega_k(t_n - \Delta \hat{t}_n)} \quad (6)$$

illustrating how the rephasing adjusts the time delay content of the received signal. At the true transmitter location \vec{x}_* (subscripted with $*$), the delays removed by rephasing are the same as the delays imparted by line-of-sight propagation, and the column vectors in D become linearly dependent,

$$\begin{aligned} S(\vec{x}_*) &= D(\vec{x}_*) + M(\vec{x}_*) \\ &= a_n e^{-j\theta_n} + M(\vec{x}_*) \end{aligned} \quad (7)$$

and thus $D(\vec{x}_*)$ is rank one. As the rephasing operation preserves total signal energy (the Frobenius norm of S), the rank structure, as described by the singular values (obtained via singular value decomposition [9]) of $S(\vec{x})$

$$U^H S(\vec{x}) V = \Sigma = \text{diag}(\sigma_1, \sigma_2, \dots, \sigma_n) \quad (8)$$

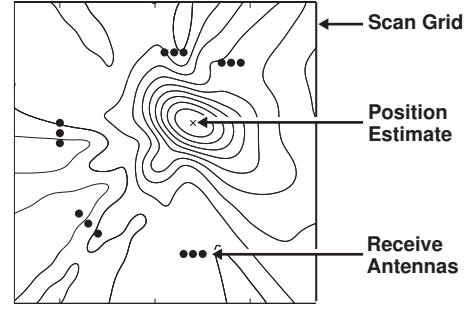


Fig. 3. Example SART image

TABLE I
LOCATION TESTING MEAN ABSOLUTE ERRORS

Test Location	Error	Bandwidth
Kaven Hall	0.37 m	60 MHz
Atwater Kent, indoor	0.71 m	60 MHz
Atwater Kent	1.08 m	60 MHz
Campus Ministry 1st fl.	0.59 m	60 MHz
Campus Ministry 2nd fl.	0.72 m	60 MHz
Campus Ministry 1st fl.	0.72 m	150 MHz
Campus Ministry 2nd fl.	0.30 m	150 MHz

reflects the distribution of received signal energy among the linearly independent basis vectors of $S(\vec{x})$. Assuming that the receivers are not overwhelmed by multipath signal energy, the first singular value σ_1 measures the strength of linear dependence between the rephased direct path signal components and is maximized at the transmitter's location. This is the SART metric.

As the SVD is a highly nonlinear operation, it is impossible to analytically estimate precisely what location would maximize σ_1 . However, the ability to evaluate the SART metric at any point in space admits to a brute-force imaging approach: by exhaustively computing and recording the first singular value of $S(\vec{x})$ over a 3-D region of space, we obtain a map of the intensity of σ_1 and may brute-force search for a maximum, whose location is chosen as the position estimate. An example SART image is shown in Figure 3, generated in simulation, showing correct determination of the transmitter's position, despite the presence of attenuative isotropic reflectors used to simulate multipath. The following section presents references to and results of experimental field tests of the SART algorithm.

EXPERIMENTAL LOCATION TESTS

Publications [1], [5] by the authors have previously presented location testing results using the SART method driven by manually surveyed receiver coordinates, and are summarized here in Table I. All results involve location of a transmitter inside the building by antennas placed outside of it, except in the Atwater Kent "indoor" case where the receiving antennas were placed completely indoors with interior walls separating the transmitter and receiver antennas. The Kaven Hall and Atwater Kent buildings are brick and steel-beam construction and comprise laboratory and office space on the

WPI campus; the Atwater Kent indoor location is an indoor-to-indoor test centered around an undergraduate computer laboratory, passing through steel-studded interior walls and near metal-corrugated ceilings; and the Campus Ministry location is a typical wood-construction three-story residential structure complete with furniture and metal appliances in the kitchen.

GEOMETRIC AUTO CONFIGURATION

Geometric auto configuration (GAC) is the process by which our location system determines, in an unattended fashion, the locations of the receiving stations. The GAC process can be divided into two parts. The first part is the determination of the geometry of the receiving stations, which is the primary challenge considered in this paper, and is solely concerned with the accuracy of their positions. The second part of GAC, not considered here, concerns the mapping of the discovered antenna geometry in a meaningful way within the context of the area of operations and conforming with the common conventions of relative and absolute position used by response personnel to enable unambiguous interpretation of location data.

It is conceivable that position and orientation information for the receiving antennas, by virtue of being mounted on fire trucks, could be obtained via GPS; however to satisfy the target system accuracy, such fixes would consistently need to achieve sub-meter accuracy. Such partial location and orientation information would aide the GAC process in narrowing the solution space for array locations and orientations and thus reduce computation time, but does not displace it.

To accomplish GAC, each of the N receiving stations are equipped with a MC-WB transmission capability. Upon arrival at an incident, the stations in turn transmit the multicarrier signal while all others receive it from their deployed locations. The receiving stations simultaneously record the signal associated with each transmitter, resulting in $N^2 - N$ unique received signals captured in total. At each transmit station, the transmitter RF input may be synchronously captured by the unused receiver, which allows measurement of the transmitter's time offset at that moment so that subsequent elimination of it in software is possible.

Figure 4 shows the typical antenna layout used for testing, with antenna positions indicated by circles. The four lines joining groups of antennas indicate that the connected antennas are considered part of the same antenna *array*, that is, they would have fixed configurations due to being permanently mounted on the same vehicle. For all processing, we assume the intra-array distances are known; this is useful as it reduces the amount of work required for a solution and because same-array antennas will have edge-on look angles to each other and likely have worsened antenna response effects in terms of high phase response distortion and reduced gain.

GAC SOLUTION METHODS

From the ensemble of interantenna signals collected, a solution for the antenna configuration may be pursued. In the following sections we present two methods: one based on

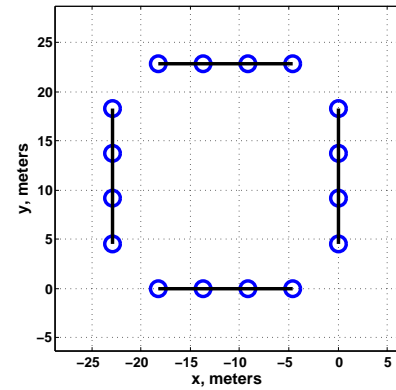


Fig. 4. General Form of Antenna Geometry

spatial scanning, and the second based on interantenna range estimation.

Spatial Scanning

The spatial scanning (SS) procedure for GAC is a direct extension of the SART method. SS builds the antenna geometry by successively scanning for each unknown array's position using signals exchanged only between that unknown array and the arrays whose positions have been determined previously within the geometry. If we denote the vector of frequency samples for an exchange between antennas i and j as $s_{i,j}$ and assume antennas 1–4 comprise array 1, 5–8 comprise array 2, etc., the first SART scan determines the position of array 2 relative to array 1 using the signals

$$S = (s_{1,5-8} \quad s_{2,5-8} \quad s_{3,5-8} \quad s_{4,5-8}) \quad (9)$$

exchanged between antennas part of arrays 1 & 2. Intra-array signals such as $s_{1,4}$ which are assumed known and hence do not vary when the position of array 2 is changed are omitted. To shorten the time needed for a scan, we assume that the position of the array is known to within a $5\text{m} \times 5\text{m}$ region. When array 2's position has been estimated, its position is fixed within the geometry and the SART matrix is altered to include signals that array 3 exchanged with arrays 1 & 2:

$$S = (s_{1-4,9-12} \quad s_{5-8,9-12}) \quad (10)$$

where $s_{1-4,5-8}$ represents sixteen data columns. This process continues until all array positions are estimated within the geometry.

For the purposes of transmitter location (not GAC) SART is fundamentally a TDOA method; as the untethered transmitter's time offset is not known, and the first term of Eq. 7 is generally a sinusoid $a_n \exp(-j\omega_k \Delta t)$ rather than constant. In GAC, this transmitter offset is captured along with signal data and is eliminated in the calibration process. Thus by taking advantage of absolute time information, the location solution may further be restricted. This is especially important because the location problem posed by GAC is more geometrically challenged (in a dilution of precision sense) as compared to the case of transmitter location estimation in which the antennas

very nearly surround the transmitter providing low dilution of precision, while during GAC, the objects being located are always on the perimeter of the geometry, and could benefit from absolute time information.

If the transmitter's time offset has been eliminated, absolute time information can be exploited by a data extension to the SART matrix which appends a conjugate (indicated by a superscript *) copy of the data columns onto the original SART matrix S :

$$S_e = (S \quad S^*) \quad (11)$$

after the rephasing step.

This stacking imposes an additional condition for *all* the columns of S_e to be linearly independent and contribute to a single singular value, and thus indicate position: that the signal delays be *absolutely* aligned by the rephasing process. When only relatively aligned, the direct path components of the two halves of S_e contribute to two separate singular values corresponding to the positive- and negative-frequency complex sinusoids:

$$(S(\vec{x}_*) \quad S^*(\vec{x}_*)) = (a_{rn}e^{-j\omega_j\Delta t} \quad a_{rn}e^{+j\omega_k\Delta t}) \quad (12)$$

which is only rank one when absolute alignment is achieved, that is, when the time offset Δt of the underlying signal data is zero. Thus the matrix extension allows a further peak in singular value when the rephased signal delays transition from relatively to absolutely aligned when indicating position.

Table II illustrates performance figures for this spatial scanning approach using experimental data collected at a number of locations with different antenna types. The Outdoor and Football field test locations were both outdoor tests on level ground with unobstructed line-of-sight between antennas; Kaven Hall is a brick, concrete, and steel-beam building; the Campus Ministry is a typical three-level wooden-frame residential structure including metal appliances in the kitchen; finally, the Odeum was an indoor-to-indoor test conducted in an empty function hall. The four "M" columns correspond to different variations in the algorithm: methods M1 & M2 use the unextended SART matrix S , while M3 & M4 incorporate the stacking matrix extension of Eq. 11; Methods M1 & M3 discover arrays by proceeding counterclockwise (i.e., 1,2,3,4), while M2 & M4 discover opposing arrays first (i.e., 1,3,2,4). While no significant difference is observed between the two orders of array initialization, stacking has lower average error across all tests.

Total System Performance

Figure 5 illustrates the result of a spatial scan compared with the manually determined coordinates from a test conducted at the WPI Odeum. In this test, three arrays were inside the function hall and a fourth was placed outside the room (indicated by a dotted line) on the other side of an interior wall. Using manually determined antenna coordinates the RMS transmitter location error for sixteen test points in the interior of the geometry was 0.18 meters. Using the GAC-determined antenna coordinates, the transmitter location error increased to 0.43 meters.

TABLE II
SPATIAL SCANNING RMS ERROR, METERS

Test Location	M1	M2	M3	M4	Antenna
Outdoor	1.78	0.72	2.17	1.82	BT-GP
Football field	4.17	2.50	0.81	0.83	BT-GP
	1.36	0.18	0.74	0.72	Bowtie
Odeum I	0.53	0.08	0.69	0.67	Patch
	1.33	1.00	1.27	0.23	Patch
	0.49	1.04	0.83	0.76	Bowtie
	2.73	2.70	1.02	1.07	BT-GP
Odeum II	0.91	0.25	0.72	0.73	Patch
	2.98	1.89	0.75	0.70	Patch
Kaven Hall	1.84	3.64	2.37	0.90	BT-GP
Campus Ministry	2.70	3.84	0.89	1.15	BT-GP
Means	1.89	1.62	1.11	0.87	

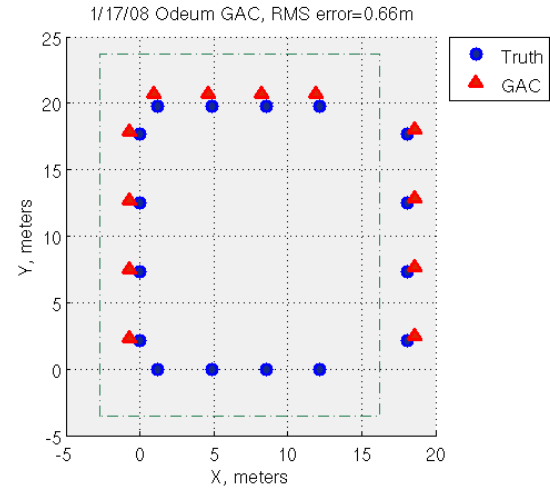


Fig. 5. Spatial Scan GAC result in Odeum

Interantenna Ranging

A second approach to GAC is to estimate the antenna positions from measurements of all interantenna ranges. While similar to the ranging approach presented in the previous paper [6], this method utilizes a SART technique for range estimation, and does not require estimation of the number of signals present nor discrimination of the direct path signal.

The approach starts by conducting a one-dimensional SART scan to determine the time delay of each signal $s_{i,j}$. Using the conjugate stacking method described in the previous section, each scan for range uses a two column SART matrix:

$$S = (s_{i,j} \quad s_{i,j}^*) \quad (13)$$

whose first singular value will peak when $s_{i,j}$ is rephased for the true time delay. When the time delay of all signals is estimated, the delays are passed as distance matrix D to a multidimensional scaling (MDS) solver which returns the desired antenna coordinates. The MDS routine used is an iterative gradient-descent solver, which allows weighting of the entries of D , missing data (signified by zero weight), and an initial solution estimate used as the starting point of iteration. As our antenna geometry is three-dimensional and we have sixteen antennas, there is redundancy in the

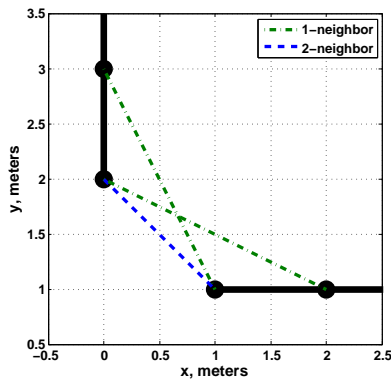


Fig. 6. Illustration of neighbor distance metric

distance information in D such that MDS may converge to a solution given many missing (or deliberately omitted) ranges. The redundancy in D may be understood geometrically by connecting line segments between the antennas of Figure 4: if the ranges to the three closest neighbors on each side of every antenna were known, then the antennas and fixed-length segments that represent the ranges form an interconnected set of rigid quadrilaterals, and thus a rigid antenna configuration with no degrees of freedom, uniquely specifying the geometry.

Due to this ability of our MDS method to converge with missing data, the following results present errors as a function of neighbor distance, as illustrated in Figure 6, which indicates the number of immediate neighbors on each side of an antenna whose range estimates are input to MDS. This is a useful parameterization as we wish to rely on range estimates between antennas who are more immediate neighbors than antennas who are further away and likely occluded by building structures.

For comparison with the results in Table II, Table III presents results from interantenna ranging tests, illustrating the best and worst performance taken over neighbor distance, achieved at each test location.

TABLE III
INTERANTENNA RANGING RMS ERROR, METERS

Test Location	Best	Worst	Antenna
Outdoor	0.20	1.86	BT-GP
Football field	0.43	0.62	BT-GP
Odeum	0.68	1.83	Patch
Kaven Hall	0.72	0.96	BT-GP
Campus Ministry	2.08	3.71	Patch
	0.80	1.90	Bowtie
Means	0.97	1.81	

Outdoor Testing

Figure 7 shows antenna location results for outdoor tests conducted without any line-of-sight obstruction. As expected, RMS antenna error is low everywhere, and the interantenna ranging approach can be said to outperform spatial scanning. The test labeled “Outdoor” was conducted using Bowtie antennas with ground planes, while the Football field tests used Patch antennas.

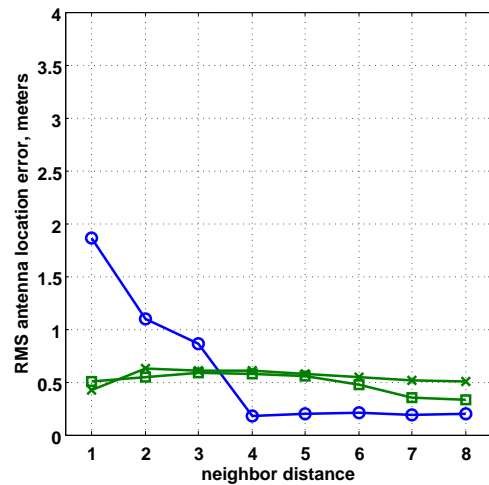


Fig. 7. Outdoor Antenna Location Error

Indoor Testing

Indoor testing serves as an intermediate step between outdoor testing and around-building testing. Figure 8 shows results from five indoor tests conducted in an empty function hall. The antennas had clear line-of-sight, but the nearby presence of building structures likely added a sufficient amount of multipath to keep the RMS antenna location error worse than the outdoor case, but below 2 meters.

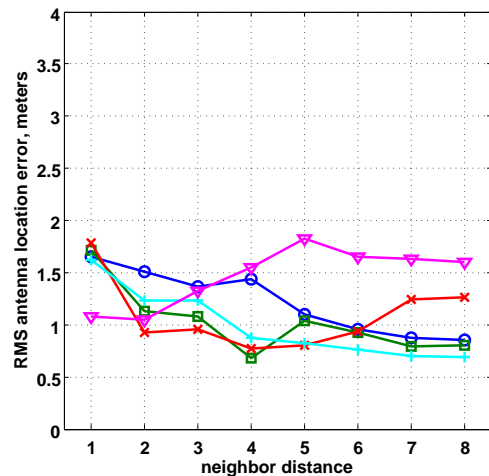


Fig. 8. Indoor Antenna Location Error

Building Testing

Around-building testing was performed at both the Kaven Hall and Campus Ministry locations. These locations featured the most realistic conditions in terms of building obstruction; Kaven Hall is a concrete, brick, and steel-beam construction building, and the Ministry is a wooden residential building complete with metal kitchen appliances. Also, the antenna geometry was truly three-dimensional, with 20 meter horizontal coverage in X and Y, and roughly 5 meter height diversity in Z. Figure 9 shows results in this case.

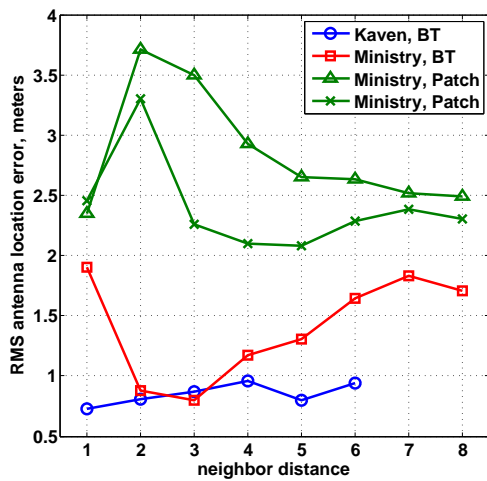


Fig. 9. Around Building Antenna Location Error

CONCLUSIONS

This paper documents a working implementation of two methods for geometric auto configuration based on the SART method for multilateralization, based on actual experimental test data. It has been shown that GAC is capable of providing near- or sub- meter antenna location performance in situations with suitable receiver geometry, even given partial data and distortion due to antenna pattern angular variation. It was also demonstrated with one example that the performance level of entire precision location system can be maintained when driven by the geometry solution methods presented.

ACKNOWLEDGMENT

The support of the National Institute of Justice of the Department of Justice is gratefully acknowledged.

REFERENCES

- [1] J. Duckworth, D. Cyganski, S. Makarov, W. Michalson, J. Orr, V. Amendolare, J. Coyne, H. Daempfling, D. Hubelbank, H. Parikh, and B. Woodacre, "WPI precision personnel locator system: Evaluation by first responders," in *Proceedings of ION GNSS*, (Fort Worth, Texas), September 2007.
- [2] D. Cyganski, J. A. Orr, and W. R. Michalson, "Performance of a precision indoor positioning system using a multi-carrier approach," in *Proceedings of the Institute of Navigation National Technical Meeting*, (San Diego, California), January 2004.
- [3] D. Cyganski, J. Orr, R. Angilly, and B. Woodacre, "Performance limits and field tests of a precision indoor positioning system using a multi-carrier approach," in *Proceedings of the Institute of Navigation National Technical Meeting*, (San Diego, California), January 2005.
- [4] R. J. Duckworth, H. K. Parikh, and W. R. Michalson, "Radio design and performance analysis of a multi-carrier ultrawideband position system," in *Proceedings of the Institute of Navigation National Technical Meeting*, (San Diego, California), January 2005.
- [5] D. Cyganski, R. J. Duckworth, S. Makarov, W. Michalson, J. Orr, V. Amendolare, J. Coyne, H. Daempfling, S. Kulkarni, H. Parikh, and B. Woodacre, "WPI Precision Personnel Locator System: Demonstrations and RF Design Improvements," in *Proceedings of the Institute of Navigation Annual Meeting*, (Cambridge, Massachusetts), April 2007.
- [6] B. Woodacre, D. Cyganski, J. Duckworth, S. Makarov, W. Michalson, J. Orr, V. Amendolare, J. Coyne, and H. Daempfling, "WPI precision personnel locator system: Automatic antenna geometry estimation," in *Proceedings of the Institute of Navigation National Technical Meeting*, (San Diego, California), January 2008.
- [7] R. F. Fahy, P. R. LeBlanc, and J. L. Molis, "Firefighter fatalities in the United States," tech. rep., United States National Fire Protection Association, June 2006.
- [8] B. D. Rao and K. S. Arun, "Model based processing of signals: A state space approach," *Proceedings of the IEEE*, vol. 80, pp. 283–309, Feb. 1992. doi:10.1109/5.123298.
- [9] G. H. Golub and C. F. Van Loan, *Matrix Computations*. Johns Hopkins Univ. Press, 3rd ed., 1996.